

Supplementary online materials for

## **Stripping back the Modern to reveal the Cenomanian-Turonian climate and temperature gradient underneath**

M.Laugié<sup>1</sup>, Y.Donnadieu<sup>1</sup>, JB.Ladant<sup>2</sup>, M.Green<sup>3</sup>, L. Bopp<sup>4,5</sup> and F. Raison<sup>6</sup>.

<sup>1</sup>Aix Marseille Univ, CNRS, IRD, INRA, Coll. France, CEREGE, Aix-en-Provence, France

<sup>2</sup>Department of Earth and Environmental Sciences, University of Michigan, Ann Arbor, MI, USA

<sup>3</sup>Bangor University, School of Ocean Sciences, Menai Bridge, UK.

<sup>4</sup>Ecole Normale Supérieure (ENS Paris) - Département des Géosciences - France

<sup>5</sup>Laboratoire de Météorologie Dynamique (UMR 8539) (LMD) - Université Pierre et Marie Curie - Paris 6, Institut national des sciences de l'Univers, École Polytechnique, École des Ponts ParisTech, Centre National de la Recherche Scientifique : UMR8539, École Normale Supérieure - Paris - France

<sup>6</sup>Total EP – R&D Frontier Exploration - France

Correspondence to: M. Laugié ([marielaugie@gmail.com](mailto:marielaugie@gmail.com))

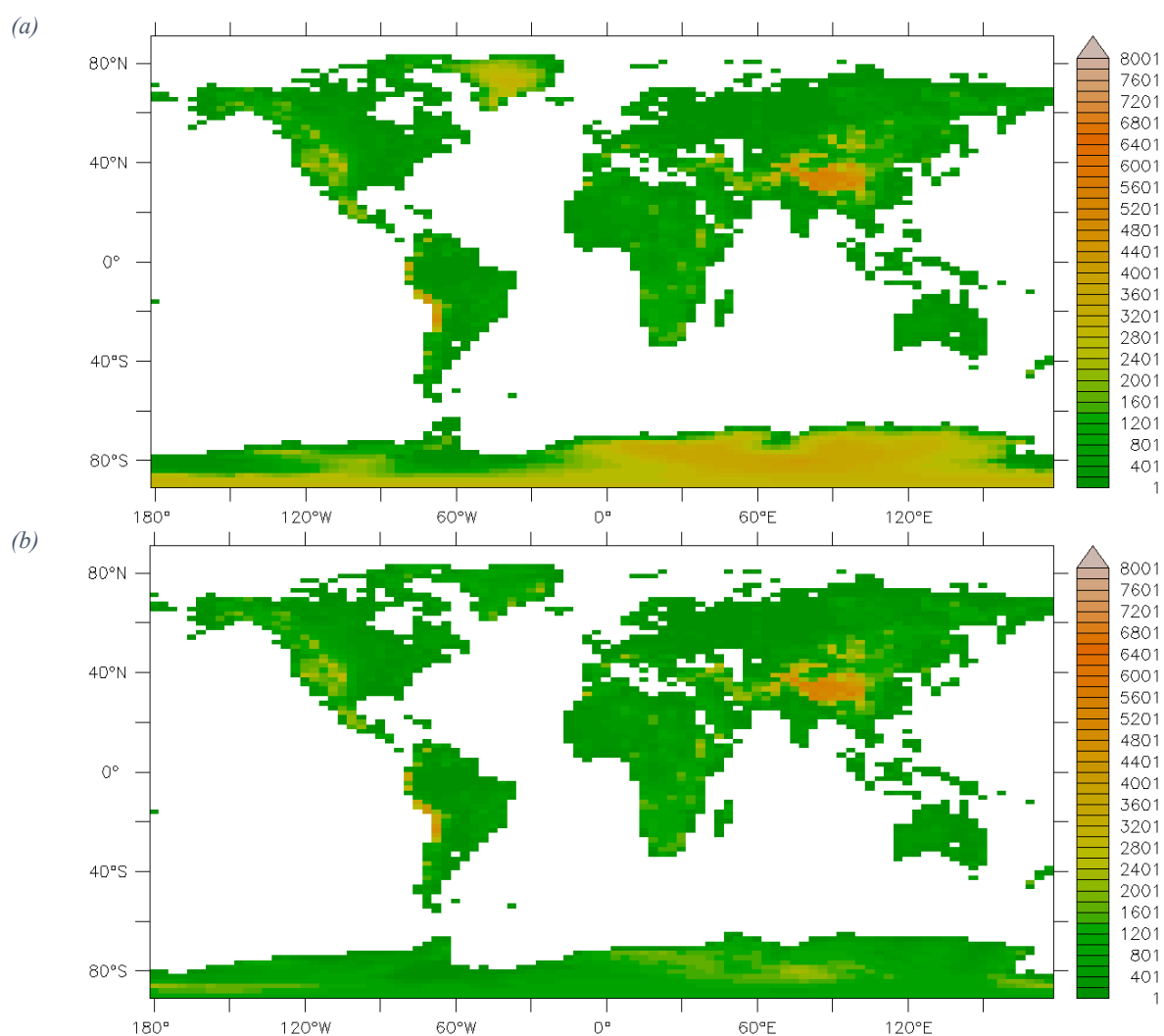
### **Contents**

- Supplementary Figures S1 to S8
- Supplementary Table S1

Table 1: Description of the PFTs and corresponding theoretical latitudinal distributions

N°	Description	Latitudinal range (North and South) and proportion
1	Bare soil	20° to 35° → 100%
2	Tropical broad-leaved evergreen	0° to 15° → 75%
3	Tropical broad-leaved raingreen	0° to 15° → 25%
4	Temperate needleleaf evergreen	Absent
5	Temperate broad-leaved evergreen	35° to 50° → 70%
6	Temperate broad-leaved summergreen	35° to 50° → 30%
7	Boreal needleleaf evergreen	Absent
8	Boreal broad-leaved summergreen	50° to 80° → 100%
9	Boreal needleleaf summergreen	80° to 90° → 100%
10	C3 grass	15° to 20° → 100%
11	C4 grass	Absent
12	C3 agriculture	Absent
13	C4 agriculture	Absent

Figure S1: (a) PiControl topography, (b) new topography accounting for isostatic rebound after polar ice cap removal and (c) corresponding anomaly. All figures are expressed in meters and shown at the LMDZ model resolution (96x96).



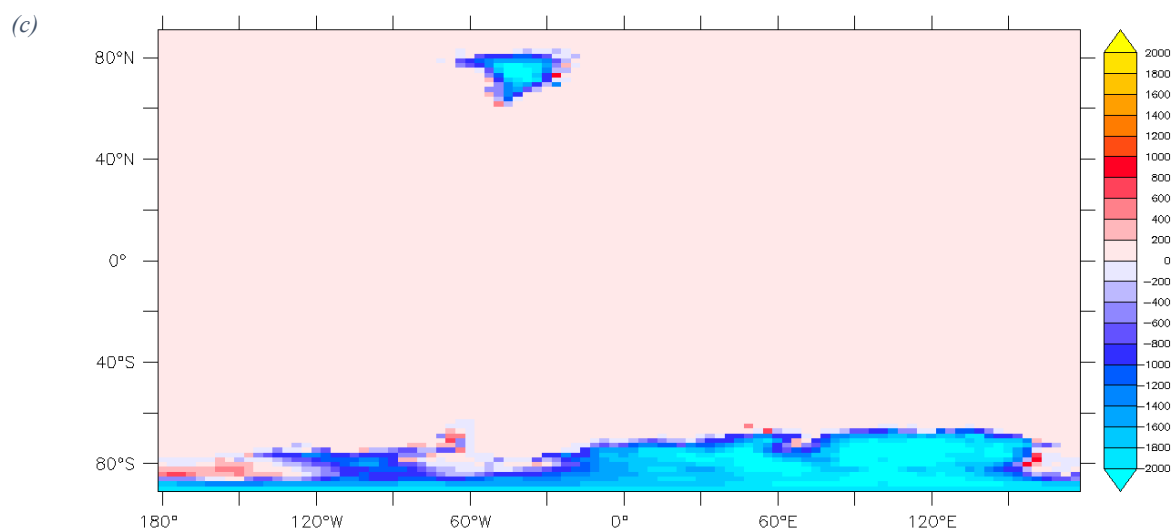
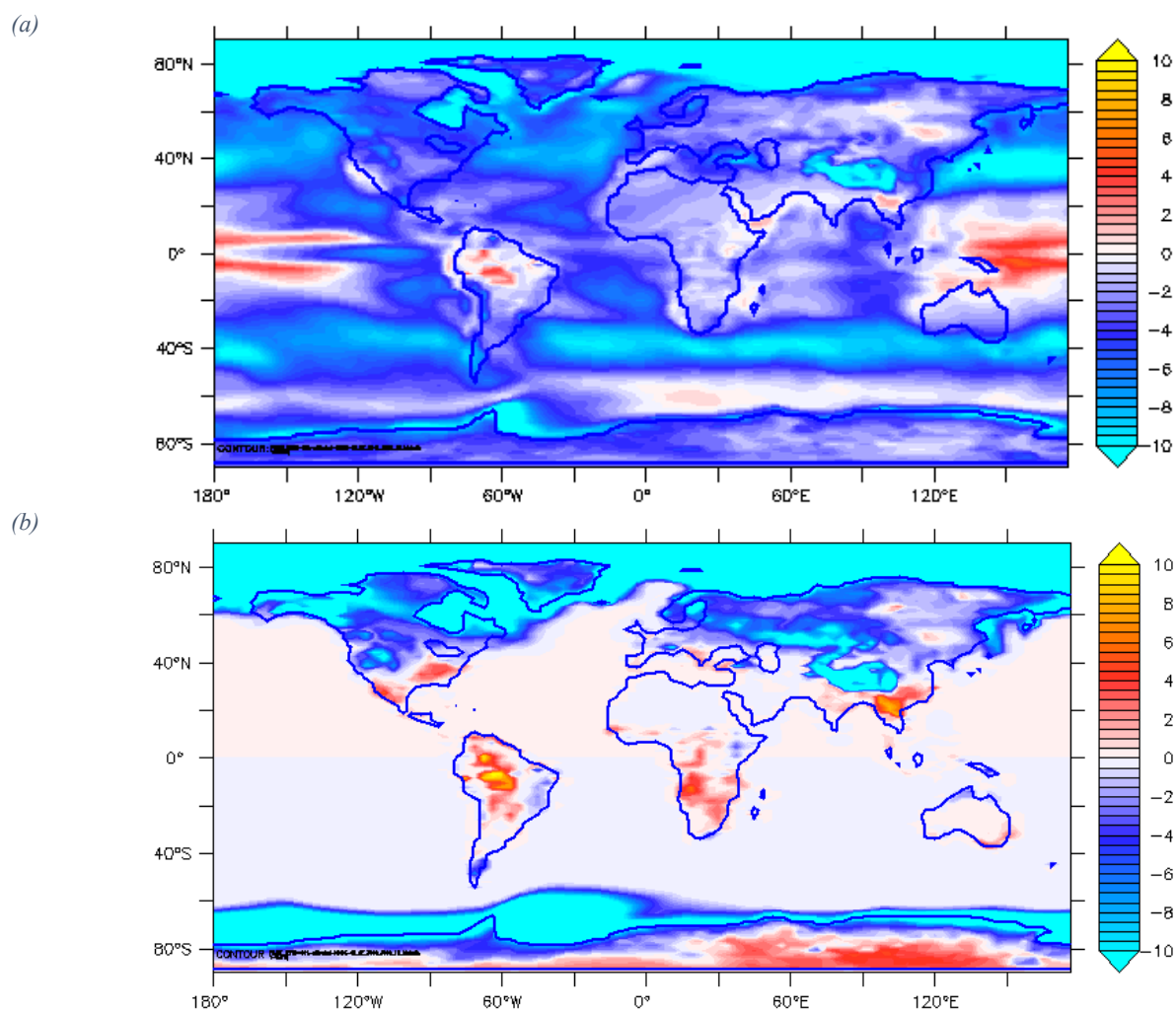


Figure S2 : Anomaly of (a) planetary and (b) surface albedo as well as (c) atmosphere emissivity between 4X-NOICE- and 1X-NOICE simulations. Units are %.



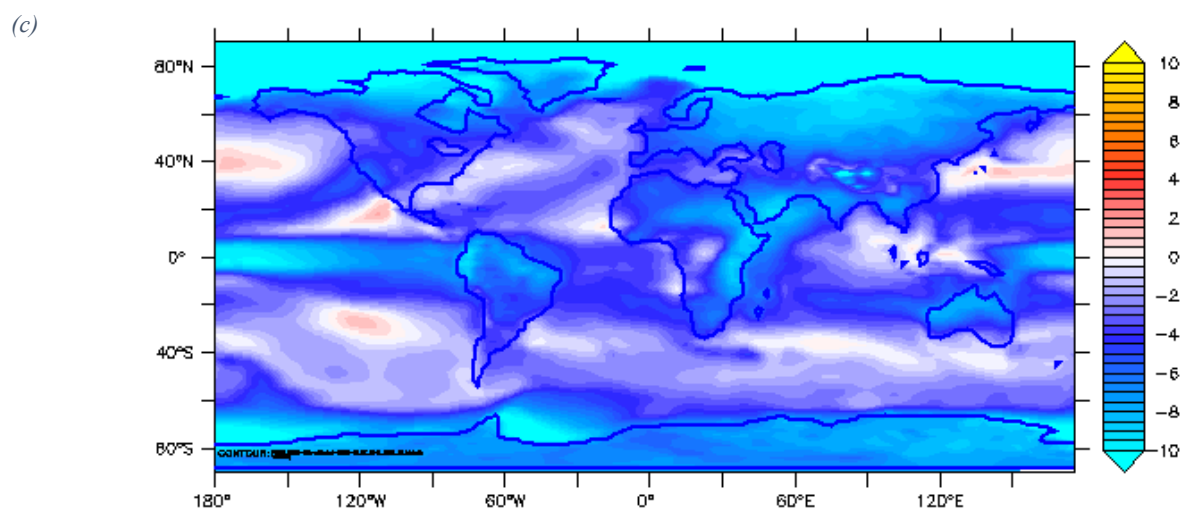


Figure S3: Anomaly of mean annual temperature at 2 meters high for 1X-NOICE and piControl simulation ( $^{\circ}\text{C}$ ) corrected with a lapse rate of  $6.5^{\circ}\text{C}/\text{km}$  in areas where topography was change after ice cap removal.

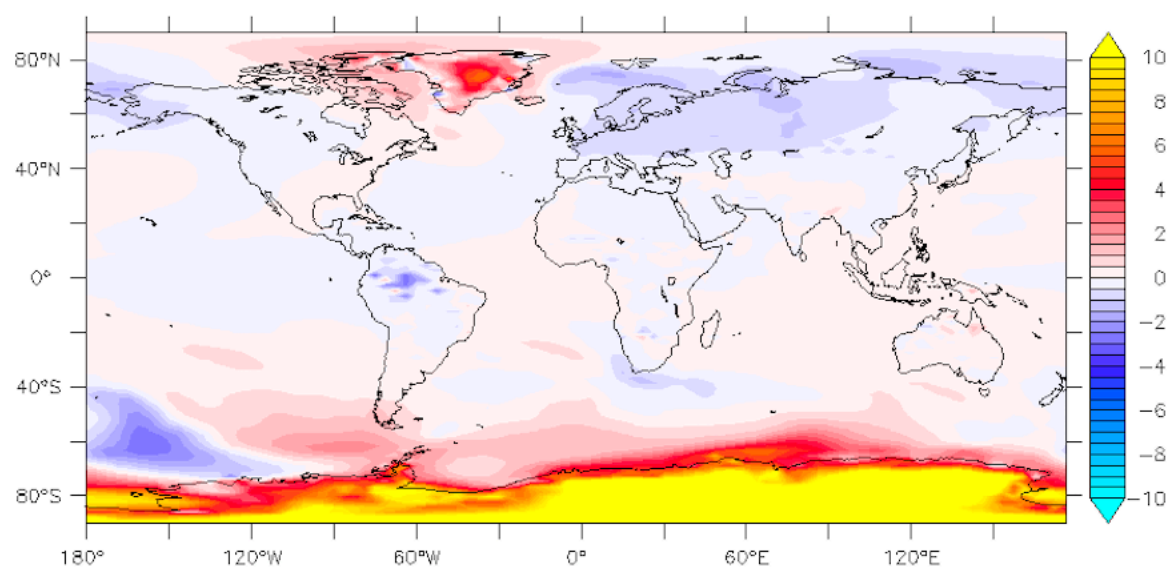
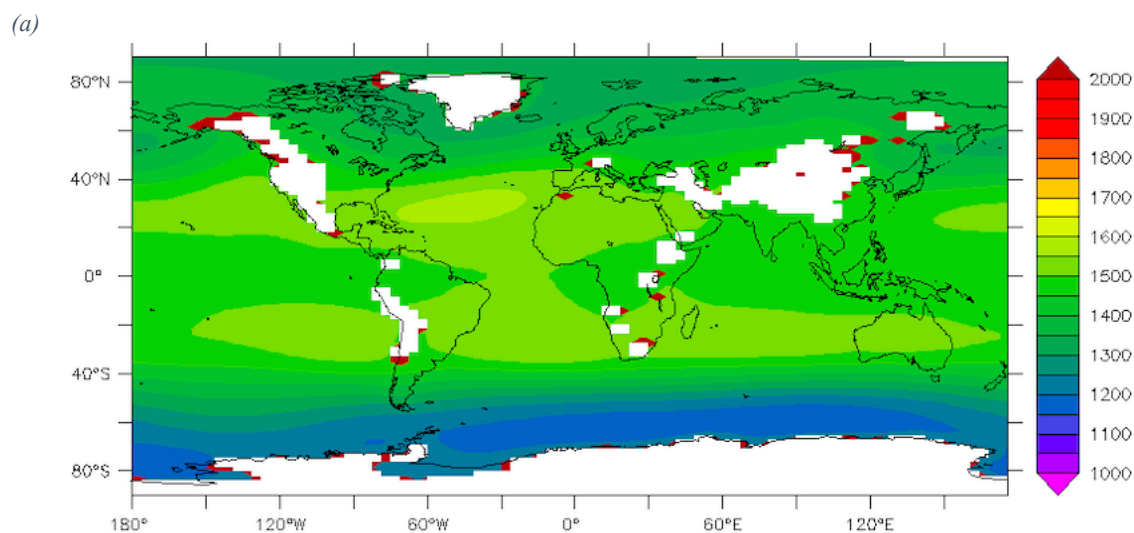
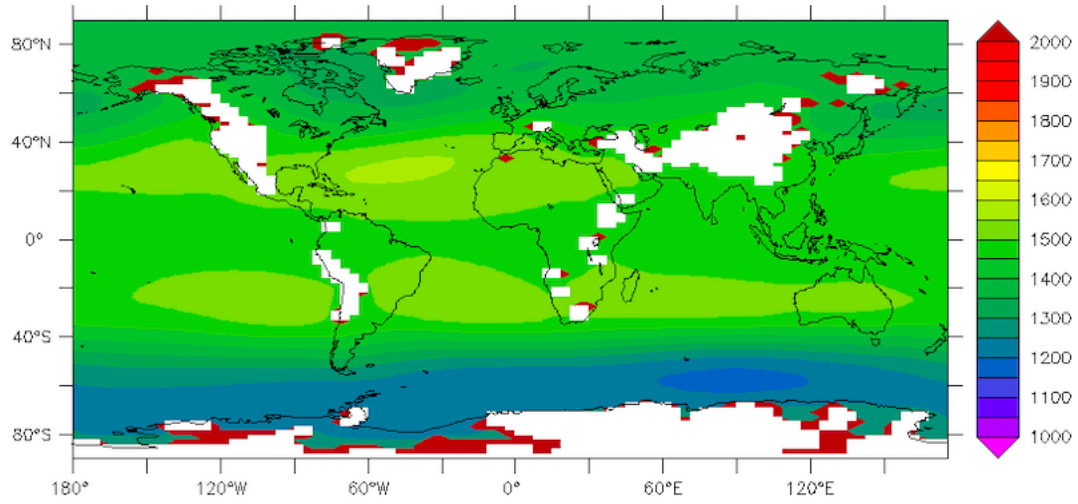


Figure S4: Geopotential height (meters) at 850 hPa for (a) piControl simulation, (b) 1X-NOICE simulation and (c) 1X-NOICE-piControl anomaly.



(b)



(c)

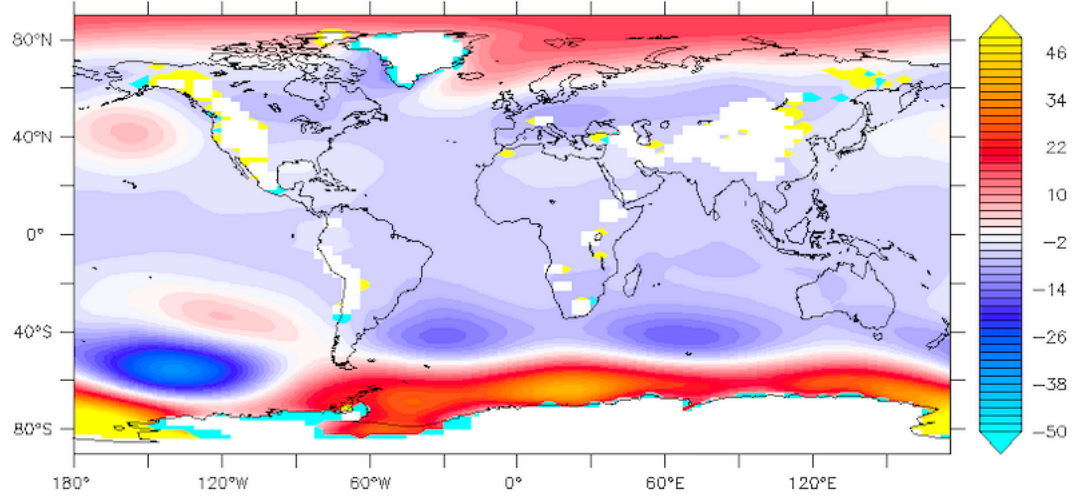


Figure S5: Zonal average of planetary albedo and atmosphere emissivity for winter and summer seasons, for 4X-NOICE-PFT-SOIL-SOLAR and 4X-CRETACEOUS simulations. The increase in albedo in the Northern Hemisphere is compensated by a strong atmosphere emissivity decrease during winter but not during summer, which leads to the seasonal pattern of cooling and warming between the two simulations. JFM = January to March, JAS = July to September

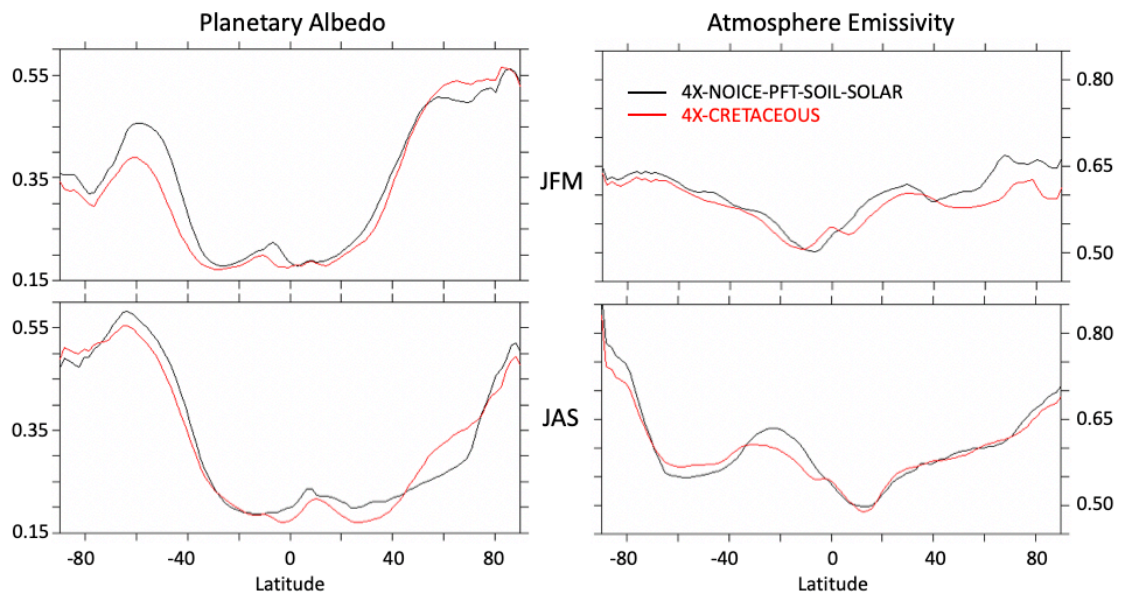


Figure S6: Barotropic stream functions for 4X-NOICE-PFT-SOIL-SOLAR and 4X-CRETACEOUS simulations.

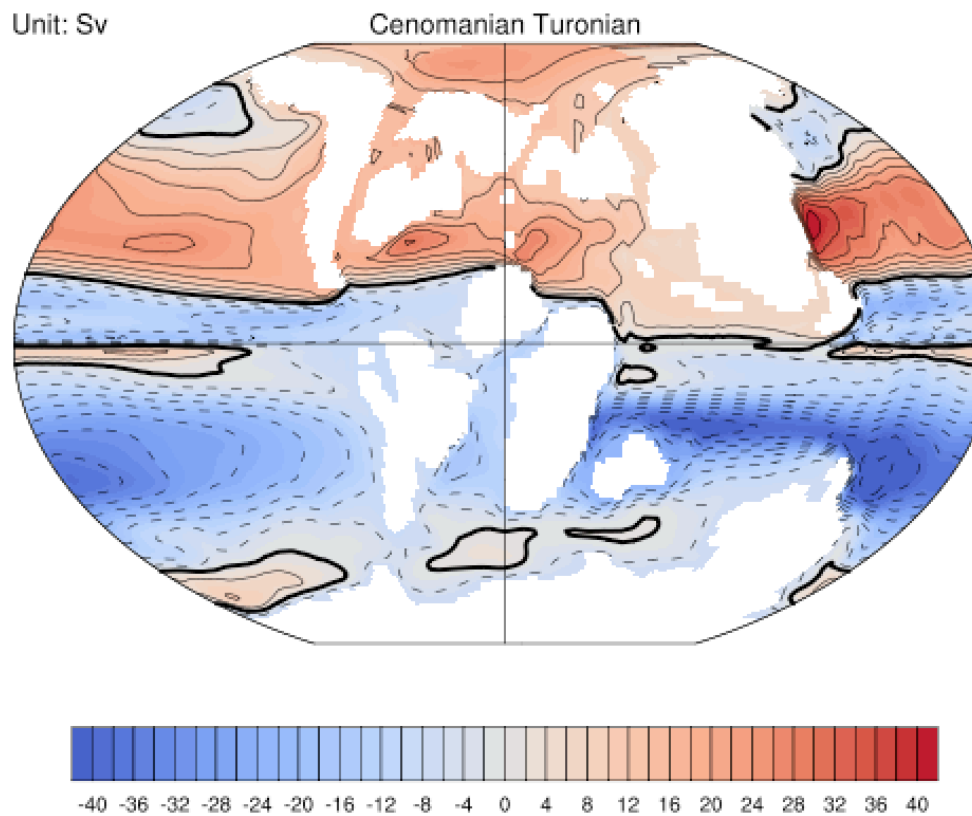
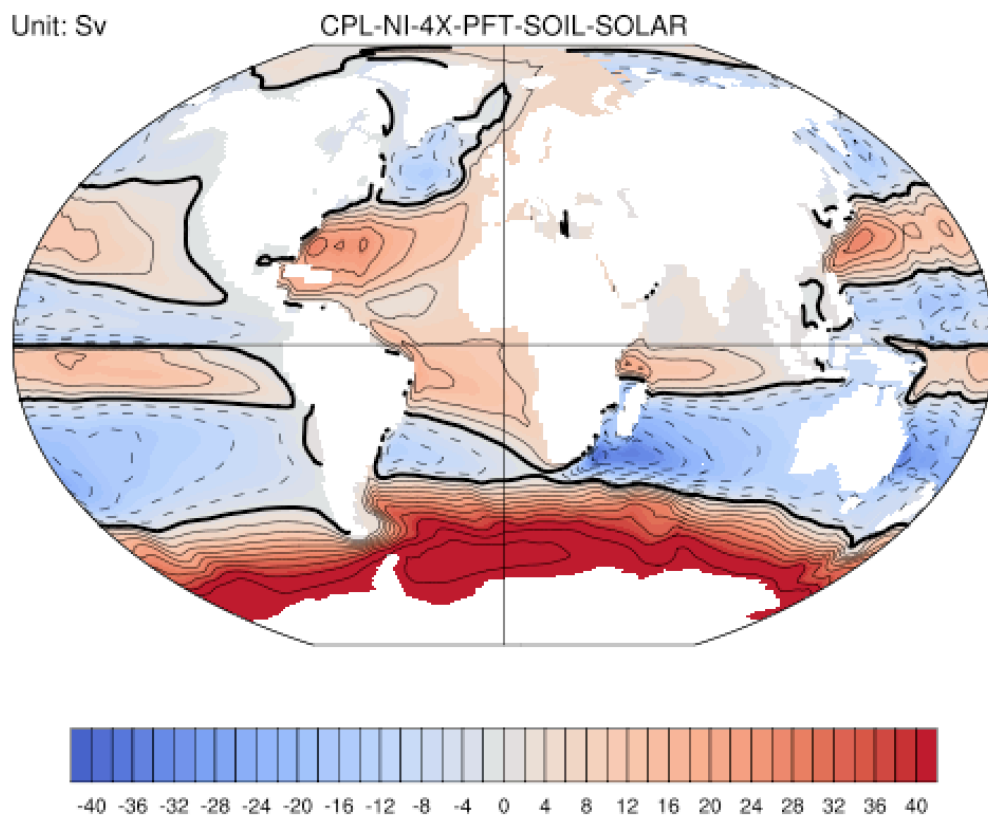


Figure S7: (a) Annual zonal average of evaporation (mm/day) for 4X-NI-PFT-SOIL-SOLAR and 4X-CRETACEOUS simulations and (b) Absolute water vapor content anomaly (annual zonal average - mL/kg) between 4X-CRETACEOUS and 4X-NI-PFT-SOIL-SOLAR simulations.

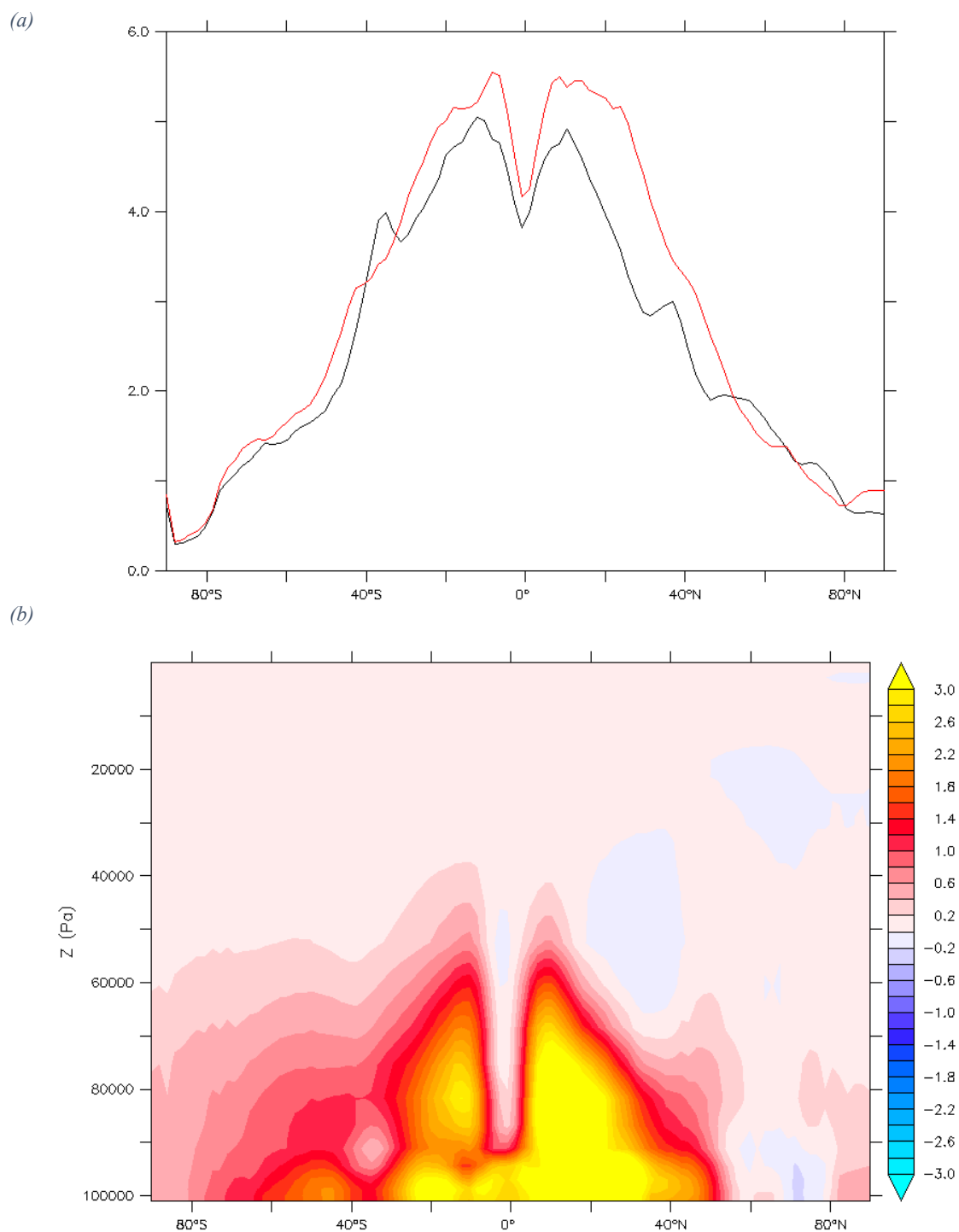


Figure S8: Anomaly of zonal annual average of relative humidity (blue curve) and low cloudiness (green curve) for 4X-CRETACEOUS and 4X-NI-PFT-SOIL-SOLAR simulations.

